UDC 551
DOI: 10.15587/1729-4061.2023.277911

DETERMINATION OF THE FATIGUE BEHAVIOR OF THE COMPOSITE SINGLE-STRINGER STRUCTURE BASED ON THE QUASI-STATIC METHOD

Ali Talib Shomran
Corresponding Author
Senior Lecturer
Department of Mechanical Equipment and Machines*
E-mail: com.ali4@atu.edu.iq

Batool Mardan Faisal
Assistant Professor
Department of Mechanical Engineering
College of Engineering
Wasit University
Wasit, Iraq, 52001

Emad Kamil Hussein
Full Professor
Department of Mechanical Power Engineering *

Thiago Santos
Lecturer
Textiles Technologies Study Group (GETTEX)
Laboratory of Knitting
Federal University of Rio Grande do Norte
Natal, Rio Grande do Norte, Brazil, 1524

Kies Fatima
Senior Lecturer
Department of Earth and Environmental Sciences
University of Milano-Bicocca
Piazza dell'Ateneo Nuovo, 1, Milan, Italy, 20126

*Mussaib Technical College
Al-Furat Al-Awsat Technical University
Mussaib, Babil, Iraq, 51006

In this investigation, the Mechanical Behavior of the composite Single-Stringer structure was subjected to numerical analysis in order to better understand its properties. As the primary material for the modeling process, the carbon-epoxy IM7/8552 with quasi-isotropic Layups has been utilized. The outcomes of the numerical analysis that were carried out on the structure while it was in its static state have been put into the structural tool that was developed by the ANSYS programme. The fundamental boundary conditions have been defined on the basis of the information that was received from the testing. Static forces with a combined magnitude of 13.7 kN are being applied to the composite Single-Stringer structure. Shear stresses, direction deformation, von mises stresses, and total deformation have all been shown to have an effect on a material's mechanical behaviour, and this effect has been demonstrated. The calculations indicate that there is a maximum amount of bending that can take place as a direct result of the load that is being applied, and that amount is equal to 0.0147. The maximum amount of bending that can take place as a direct result of the load that is being applied is equal to 0.0147. As a consequence of the application of 13.7 kN of pressure, the von Mises stress, which is also frequently referred to as comparable stresses, has reached 51.9 MPa. Shear stresses have been estimated in three distinct plans, and it was discovered that the shear stress that was applied to the XY plane achieved a maximum of 15 MPa, but the shear stress that was applied to the XZ plane reached a maximum of 9.8 MPa. This was found. Both aeroplanes were put through precisely the same amount of tension at the exact same time. At this time, the shear stress on the plane YZ has reached a level of 1.5 MPa

Keywords: directional deformation, shear analysis, general deformation, equivalent stresses, composite structure

Received date 08.02.2023
Accepted date 17.04.2023
Published date 30.04.2023

***How to Cite:** Shomran, A. T., Faisal, B. M., Hussein, E. K., Santos, T., Fatima, K. (2023). Determination of the fatigue behavior of the composite single-stringer structure based on the quasi-static method. Eastern-European Journal of Enterprise Technologies, 2 (7 (122)), 15–23. doi: https://doi.org/10.15587/1729-4061.2023.277911*

1. Introduction

Composite stiffened panels are widely used in today's thin-walled aeronautical components, including the fuselage and wing structures. Adhesive bonding or co-curing is frequently used in these buildings to secure the stringers to the skin. The bending stress that causes things to buckle.

The load that can be applied to structures is much less than the load that will cause them to fail [1]. However, the out-of-plane displacements that can take place in the post-buckling phase have the potential to become rather significant at some points. In addition, the repetitive character of these displacements might cause a separation to occur in the interface that is established between the skin and the stringer if it is not carefully monitored. Because there are no reliable numerical techniques available that are able to correctly foresee this phenomena, it is required to include the buckling load as the limit load during the design phase for aerospace stiffened panels. This is due to the fact that including the buckling load as the limit load is necessary. If the structure were to be allowed to buckle under specific well-defined service conditions, the consequence would either be an increase in the load carrying capability of the structure or a reduction in the weight of the structure when it was subjected to the same limit load. Both of these outcomes are possible. To stop the panel from failing before its time, it is necessary to pay special attention to the process of fatigue delamination start and spread. Only then will you be able to stop it from failing prematurely. The anticipated rate of fatigue delamination dissemination in post-buckled reinforced composite panels is still an unresolved issue, despite extensive investigation at the coupon level. This is because no one has found a satisfactory solution to the issue. The power law proposed by [2–4] characterizes the rate of delamination growth under fatigue loading circumstances by relating the crack growth rate to the stress intensity factor, or, equivalently, the energy release rate. This law connects damage mechanics with fracture mechanics by relating the rate at which energy is liberated through crack propagation. All of this is carried out in accordance with the Paris law and the numerical representation of delamination.

Within the realm of damage mechanics, simulations of delamination onset and propagation under quasi-static and impact stress circumstances have seen widespread adoption of interface elements that include an embedded cohesive law [5]. As a result of the positive findings gained for these issues, a select group of writers has extended the cohesive formulation in order to mimic the growth of fatigue cracks. However, the energy release rate is not directly described within the cohesive law. As a result of this, a range of models has been developed that relates the cohesive damage variable to the crack growth rate defined by [6, 7]. The vast majority of these models produce accurate findings when assessing the propagation of fatigue cracks in small samples or coupons. However, due to the enormous number of interface pieces needed to correctly depict the fatigue cohesive zone, they are impractical when applied to more complicated structural problems. This limits their usefulness for solving more advanced structural issues [8].

Numerical methods from the field of fracture mechanics, on the other hand, rely on a combination of the Virtual Crack Closure Technique (VCCT) and an energy release rate estimation methodology based on the Paris law. [9]. These approaches are referred to as "fracture mechanics-derived numerical approaches." This methodology, which was developed for modelling delamination propagation under quasi-static load circumstances [10], is now being incorporated into a number of other commercial Finite Element (FE) programs.

Because of the challenges involved in managing and forecasting the complex failure mechanisms of composite structures, the promise of composite structures in the aerospace industry has not yet been completely explored [11]. In the post-buckling era, this is truer than ever. Typical aeronautical composite stiffened panels can operate in the post-buckling regime, but it's hard to foresee how they'll fail. This is because it is difficult to forecast their mechanism of collapse because the post-buckling deformation interacts with many failure modes like intralaminar damage, delamination, and skin-stringer separation [12]. Fatigue loading conditions further complicate the phenomenon due to interactions between geometric nonlinearities of the response, different damage modes, and the accumulation of cyclic damage. This is due to the cumulative nature of damage [13].

One of the worst forms of damage in stiffened panels is delamination, especially when it takes the form of skin-stringer separation. This is because delamination can spread rapidly under favourable conditions and is hard to forecast [14].

Despite the abundance of research, it is unclear how well it is possible to simulate interlaminar damage in composite structures that have been subjected to fatigue strain. The growth of delamination is typically viewed as a problem similar to that of crack propagation, and the majority of the currently available numerical methods make use of methodologies that were initially developed for use with metallic materials. Examples include the [15], which is used to characterize experimental data in terms of fracture growth rate versus variation in energy release rate or stress intensity factor under load [16]. In order to include the Paris law within the framework of a Finite Element (FE) analysis, many different numerical techniques have been developed over the past few decades. Several methods have been used to achieve this goal. Applying the Paris rule to the VCCT has allowed several authors [17] to calculate the energy release rate and, thus, the crack propagation rate. Preliminary testing has indicated that the recently introduced approach in the finite element code ABAQUS can accurately analyze fatigue-driven delamination at the coupon level [18]. Cohesive Zone Model (CZM) methods, on the other hand, place interface elements along the surface in the direction of the crack's expected growth. Delamination simulation in composite laminates subjected to static or impact loads [19] has benefited greatly from CZM-based approaches. Some authors have subsequently expanded on these methods by include the Paris law within the cohesive constitutive model [20], thereby making it possible to account for degradation due to the cyclic load.

Therefore, numerical analysis that is devoted to determine the fatigue behavior of composite single-stringer construction based on the quasi-static approach scientific relevance.

2. Literature review and problem statement

In the mechanical sector, the full potential of composite structures has not been realized because of the challenges in managing and predicting their complex failure modes, especially in the post-buckling regime. The combination of the effects of post-buckling deformation when with various failure modes, such as intralaminar damage, delamination, and skin-stringer a division [21], makes it extremely challenging to predict the collapse mode of typical aeronautical composite stiffened panels. At fatigue loading conditions, the phenomena becomes even more convoluted due to the interplay between geometric nonlinearities of the response, the various damage types, and the accumulation of cyclic damage. One of the most serious forms of damage in stiffened panels is delamination, especially skin-stringer separation, because it is hard to foresee and can spread rapidly in favourable conditions. After numerous investigations, it remains unclear how to model interlaminar degradation in composite structures under fatigue stress. Most existing numerical approaches treat delamination growth as a crack propagation problem, and many of these methods were developed for use with metals. In order to define experimental data, the Paris law [11] is frequently used to the relationship between the rate of crack formation and the variation in energy release rate or the stress intensity factor across the load cycle. Many alternative numerical algorithms have been developed over the past few decades to incorporate the Paris law within the framework of a

Finite Element (FE) analysis. In order to determine the crack growth rate in accordance with the Paris law, several authors [22] have utilized the VCCT to determine the energy release rate. This approach, which has only recently been implemented in the ABAQUS FE code [23], has shown to be effective in assessing fatigue-driven delamination at the coupon level. Cohesive Zone Model (CZM) techniques, on the other hand, make use of interface features located along the surface where the fracture is anticipated to form. The Paris law has recently been incorporated into the cohesive constitutive model, allowing some authors to extend CZM-based techniques to simulate degradation due to cyclic stress. This is because delamination in composite laminates subjected to static or impact pressures has been frequently simulated using CZM-based techniques [24]. The so-called "envelope load method" is commonly used to apply VCCT and CZM approaches in crack propagation simulation under constant amplitude fatigue loading circumstances.

However, the Virtual Crack Closure Technique (VCCT) [25] is one example of a numerical approach that originates in fracture mechanics and relies on the direct application of the Paris law in tandem with a methodology for the estimation of the energy release rate. This method, first created to model the spread of delamination under quasi-static loads, is now incorporated into a number of widely used FE software packages. The orthogonality problem between the crack front and the structural mesh, as well as the difficulties of simulating the bi-material interface, have both been identified and addressed by numerous researchers in a wide variety of works [26]. Although this method currently provides a workable option for simulating fatigue crack propagation in structural components, it has severe limitations when dealing with fatigue delamination challenges and requires an initial damage. The goal of this study is to use the recently adopted VCCT based approach in the FE Code ABAQUS to analyze the delamination growth behaviour of a composite single-stringer specimen subjected to cyclic stress in the postbuckling regime. In this investigation, the behaviour of large multi-stringer panels, such as those present in aircraft fuselage constructions, is mimicked using a Single-Stringer Compression (SSC) specimen that was created and validated in [27]. The coupon specimen level of the building block approach commonly used for aerospace composite constructions and the large multi-stringer stiffened panel level both accommodate the specimen. The SSC specimen is small and cheap to manufacture, but its complex framework is comparable to that of multistringer panels.

All this allows to assert that it is expedient to conduct a study on research utilizing numerical analysis have been evaluated in order to investigate the mechanical behaviour of the composite structure of the Single-Stringer structure utilizing an approach that is regarded as being quasi static.

3. The aim and objectives of the study

The aim of the study is to determination the mechanical behavior of the composite single-stringer structure based on the quasi-static method.

To achieve this aim, the following objectives are required:

– to calculate total deflection based on the quasi-static method;

– to calculate directional deflection based on the quasi-static method;

– to measure the value of von Mises stress;

– to investigate the influence of shear stresses.

4. Materials and methods

4. 1. Object and hypothesis of the study

Object of the study is fatigue value the composite Single-Stringer structure's.

The GoodMan concept has been taken into account in the computations that have been done as part of this investigation. In order to carry out the simulation technique, which is dependent on the static structural modelling, the software known as ANSYS has been utilized.

4. 2. Physical and mechanical properties of the composite Single-Stringer structure

The surface is constructed out of 8 unidirectional plies of carbon-epoxy IM7/8552 with a quasi-isotropic layup, while the stringer is constructed out of 7 plies with a layup. Even though the material system is the same as that of the MMB specimen that was examined in the previous section, the properties that were reported in [21] and those that were shown in Table 1are slightly different from one another. This numerical simulation uses the material properties that are outlined in Table 1.

Table 1

Physical and mechanical properties of the composite Single-Stringer structure

Property	Value	Unit
Modules Modulus of Elasticity	44	MPa
Density	2.2	(g/cm^3)
Passion ratio	0.32	Unitless

Physical and mechanical properties of the composite Single-Stringer structure have been calculated to be used as a primary boundary condition accordingly.

4. 3. Geometry and mesh

The geometry of the single plate has been performed and investigated statistically using AutoCAD software. The middle section is separated from the rest of the plain section.

ANSYS Mesh generation was used to complete the meshing process for this particular problem. Mesh generation reduces the number of particles in a model from an indefinitely large number to one that is more manageable. In order to get reliable results, a fine mesh was developed using a predefined grid layout. This allowed for the production of the mesh. By carefully controlling the size of the curvature with a coarse mesh and the element size with face meshing, we were able to get the desired outcome of a tiny mesh. This made it possible to get the desired result of a tiny mesh. The formation of binary nodes for the wedge across all of its zones has resulted in a grand total of 553345 binary nodes. Illustration of this form of mesh in a two-dimensional environment is shown in Fig. 1. Given the symmetry of the 3D wedge, this is the only aspect of the model that has been worked on and modeled so far. This is due to the serendipitous discovery of the symmetry of the 3D wedge. The authors of this work employed wedge boundary conditions, symmetric boundary conditions, and far field boundary conditions in their research. These constraints emerged from mining the model for edges to employ in the selection procedure.

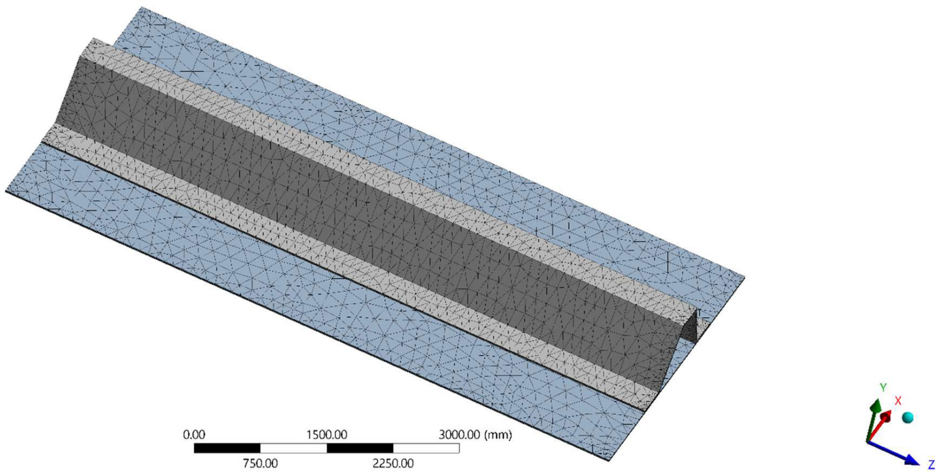

Fig. 1. Meshed model of the composite single-stringer structure

4. 4. Convergence process

In the study conducted that has been carried out, the total deformation has been taken into consideration as the key indicator for the convergence technique of the composite single stranger plate. Convergence process was carried out as a part of an attempt that was being made to gain a better understanding of the convergence method. To the point when it converges on a deflection of 3.32e5 mm, the mesh that represents the existing geometry has been refined to the point where it can now accurately describe the geometry. Fig. 2 shows that the minimal amount of deviation required for convergence is 2.9e5. This can be seen by looking at the graph. The Fig. demonstrates this point quite clearly. Following the successful completion of that multi-step procedure, the von Mises stress, shear stresses, and any other relevant parameters can be applied in the manner that is most appropriate.

The analysis of the nodes and elements has also been explained, and it can be shown in Fig. 3. There are three different approaches that have been tested in order to find the optimum combination of elements and nodes. The current iteration of the simulation procedure has been carried out while taking into consideration the third option. The point at which the total number of elements reached 69294.

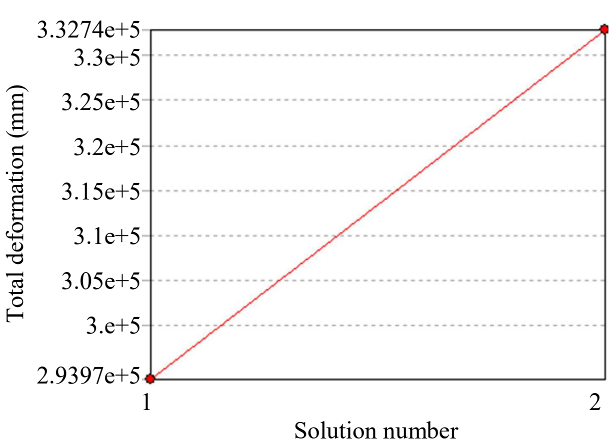

Fig. 2. Convergence process of the current study

The nodes and elements of the mesh have been determined with the help of the statistics of the mesh. In order to complete the simulation procedure, three distinct solutions have been computerized and analyzed.

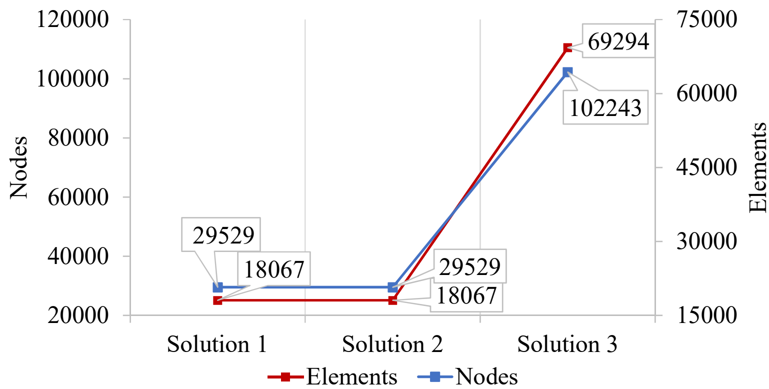

Fig. 3. Elements and nodes with final solutions

5. Results of the investigation of the mechanical behavior of the composite single-stringer structure based on the quasi-static method

5. 1. Total deflection based on the quasi-static method

The quasi-static method was utilized in order to analyze the whole deflection that was produced by the 13.7 KN load that was supplied to the single stringer plate during the research process. The absolute maximum, as determined by the outcomes of the computer simulation, is 0.0147 millimeters. The explanation that was supplied by the simulation revealed that the edge of the plate that is parallel to the horizontal plane is the location of the maximum deflection that occurs as shown in Fig. 4, *a*, *b*.

Only the effect of the force on the plate as measured in terms of its deflection is shown in Fig. 5. The location at which it is believed that the *XZ* plane is displayed. The findings of the numerical analysis showed that the Single-Stringer structure exhibited the greatest amount of deflection in response to the applied loads along the horizontal border of the plate as well as in the central portion of the plate. Fig. 5 shows the iso lines of the deflection distribution based on the applied load.

According to the findings of the Total deformation study, the only part of the composite Single-Stringer construction that has been investigated is the plate. 0.0147 mm is where the greatest value of total deformation can be found.

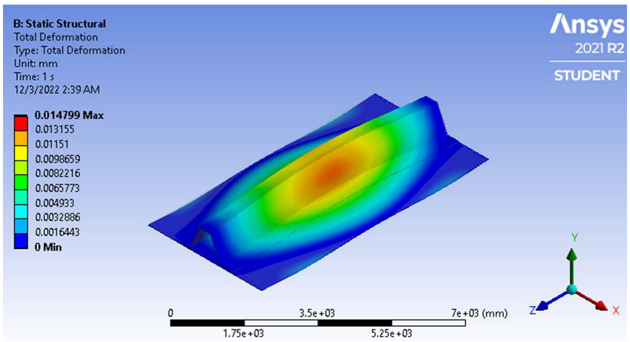

a

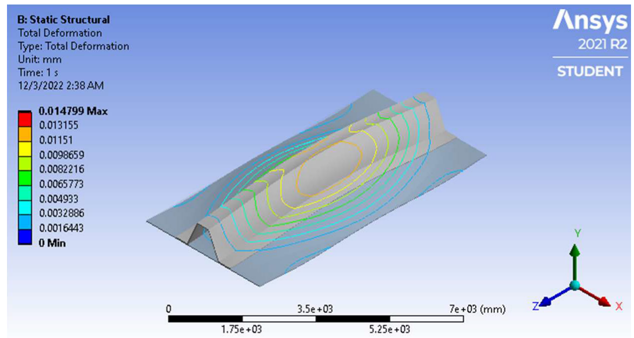

b

Fig. 4. Total deformation of the composite Single-Stringer structure due to the applied load: *a* – graphical explanation; *b* – isoline explanation

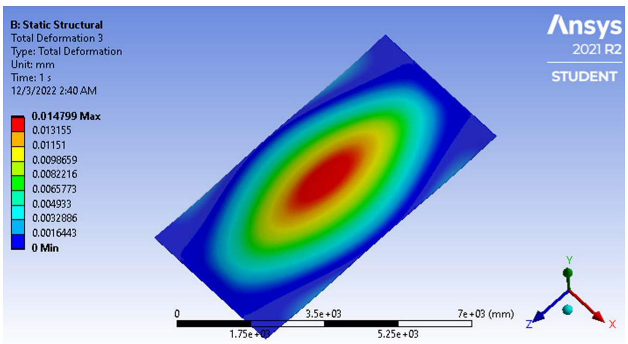

Fig. 5. Total deformation of the only plates of the composite Single-Stringer structure

5. 2. Directional deflection

Fig. 6 illustrates the directional deflection that occurs in each of the three directions as a result of the 13.7 KN of force that is applied. This deflection can be observed as a result of the application of the force. It was anticipated that both the maximum value for the deflection in the direction *Z* and the maximum value for the deflection in the direction *X* would be 0.0091 mm, and we have already reached the maximum value for the deflection in the direction *Y*. As a consequence of this, three curves were utilized in order to explain the deflectional behaviour of the composite Single-Stringer structure in a quasi-static approach.

Calculations of deformation have been done in all three directions (x, y, and z). According to the findings, the highest possible value of deformation was seen in the *Y* direction.

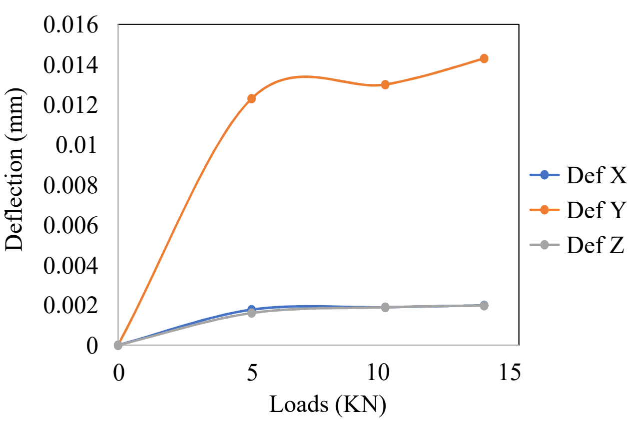

Fig. 6. Directional deflection respected in all directions

5. 2. 1. Directional deflection at X

The graphical illustration of the deformation as seen from the *X* direction is displayed in Fig. 7. The greatest load that may be applied is 13.7 kN. This force has been exerted in a vertical direction while maintaining its consistency. The simulation was carried out utilizing the static structural tool that is included in the Ansys R1 version. It was done so in accordance with the global coordinate system (GCS). According to the process of simulation, the highest amount of plate deflection in the *X* direction has reached 0.001985 mm in the middle of the plate, while the minimum amount of plate deflection has reached –0.00199 mm at the plate's edge. Fig. 7, *a*, *b* illustrates the location of the plate's deflection as well as the effect that the applied forces have on the plate. The effect of the deformation is depicted as an isoline in Fig. 7 so that it may be explained and understood, and the particular location of the areas that have been deflected is made obvious.

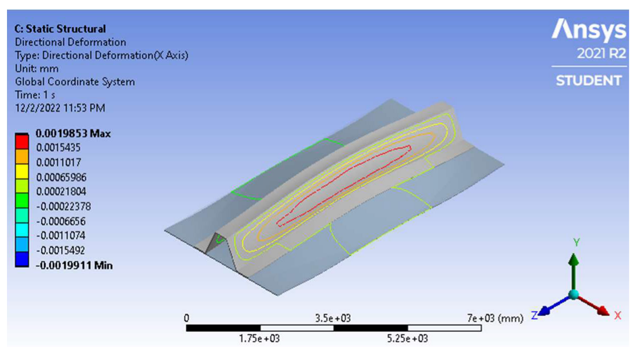

a

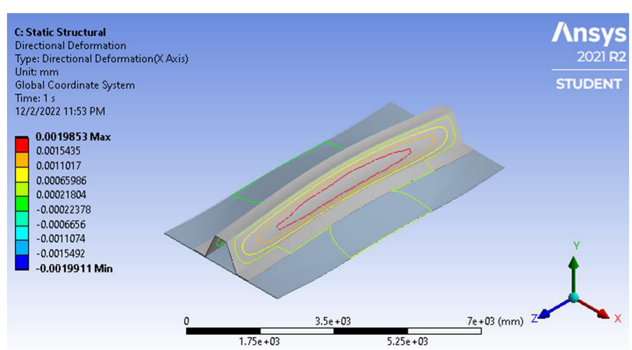

b

Fig. 7. show directional deformation at *X* direction: *a* – isoline explanation ; *b* – graphical explanation

5. 2. 2. Directional deflection at *Y*

Fig. 8 is a graphic representation of the deformation along the *Y* axis. A maximum force of 13.7 kN can be exerted. All along, this force has been consistently applied vertically. For this simulation, let's use the static structural tool in Ansys R1. And it was all done using the international system of coordinates (GCS). The simulation method shows that the plate has deflected an extreme 0.0143 mm in the *X* direction at the plate's center and a minimum of –0.00199 mm at the plate's periphery. Deformation of the plate and its relationship to the applied forces is shown graphically in Fig. 8 (AB). In order to better explain and comprehend the effect of the deformation, the isoline displayed in Fig. 8 has been drawn to highlight the precise location of the portions that have been deflected.

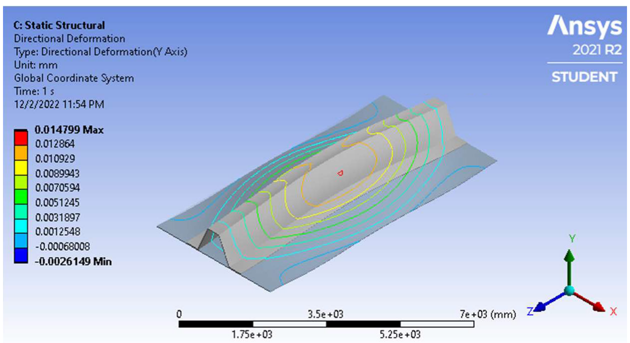

a

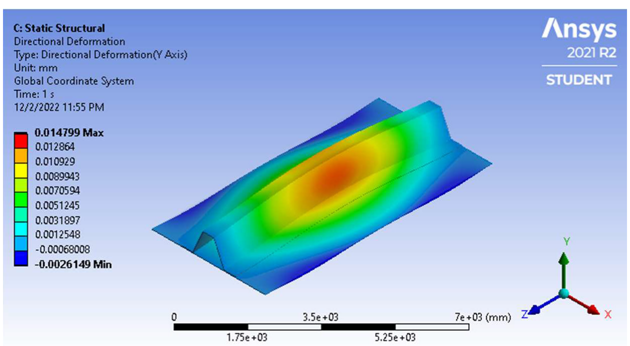

b

Fig. 8 Shows directional deformation at the Y direction : *a* – isoline explanation; *b* – graphical explanation

5. 2. 3. Directional deflection at *Z*

Fig. 9 shows a graphic display of the deformation as seen in the *Z* direction. There is a maximum allowable force of 13.7 kN. This consistent force has been consistently applied in a vertical direction. Static structural tool in Ansys R1 was used to run the simulation. These adjustments were made using the universal reference frame (GCS). Calculations show that the maximum *X*-axis deflection of the plate is 0.00197 mm at its center and the minimum is –0.00199 mm at its periphery. The location of the plate's deflection and the effect of the applied forces are shown graphically in Fig. 9, *a*, *b*. Deformed areas and their new positions are clearly shown in Fig. 9 as an isoline, making the effect of the deformation easier to describe and comprehend.

The results of the simulation led to the conclusion that the directions of deformation in three different directions should be considered correspondingly.

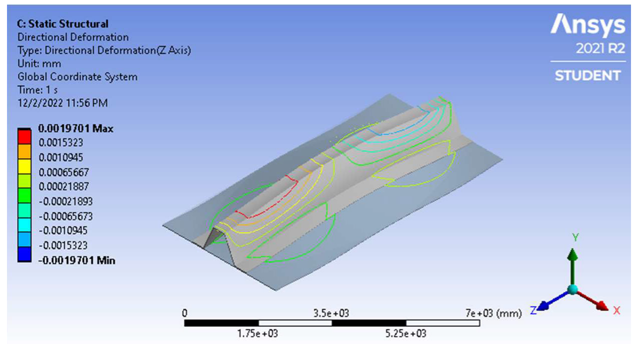

a

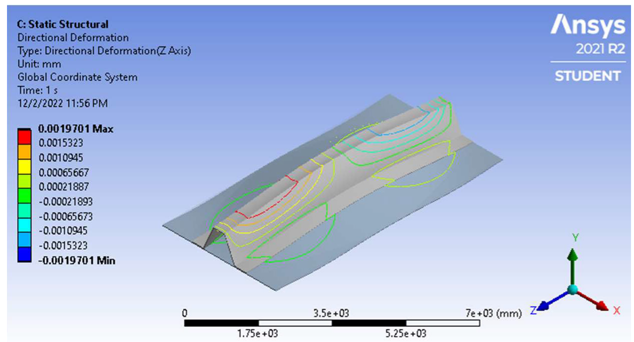

b

Fig. 9 Show directional deformation at Z direction: *a* – isoline explanation ; *b* – graphical explanation

5. 3. Criterion of von Mises stress

A graphical representation of the effect that von Mises stresses have on the Single-Stringer structure may be found in Fig. 10. The equivalent von Mises stresses concentrate on the middle section of the structure, which is why that section deflects less than the rest of the structure because of the geometry. According to the results of the simulation, the shear stress is substantially higher near the edge of the structure's core portion than it is in any other region of the structure. This is the location within the structure that has been identified as having the highest shear stress. The current location of the camera in relation to the *XZ* plane in terms of the global coordinate system. The highest value of stress, which was 51.9 MPa, was finally reached as a result of the static load of 13.7 kN that was applied to the specimen.

Fig. 11 illustrates how the comparable von mises stress acts on a single stringer plate as a result of the applied static loads represented as isolines. Isolines have the ability to clearly depict how the load is distributed throughout the plate.

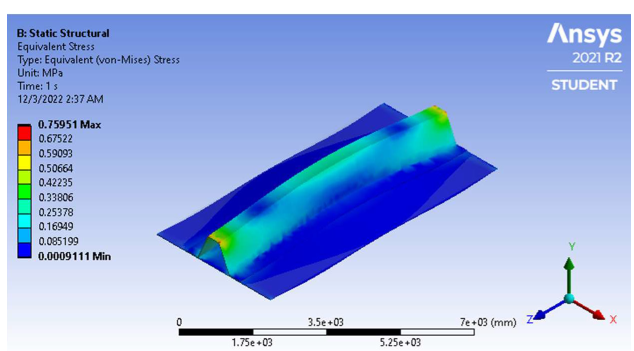

Fig. 10. von Mises stresses on the plate

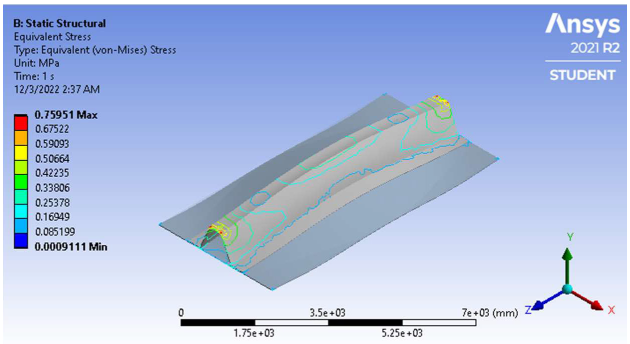

Fig. 11. Isoline illustration of von Mises stresses on the plate

The isoline illustration of von Mises stresses on the plate has been shown so that the location of the stress that has occurred as a result of the applied load may be identified.

5. 4. The influence of shear stresses

The forces that were provided as a basis for the calculations and studies that were carried out as illustrated in Fig. 12 have been used for the calculations and studies that have been carried out regarding the effects of shear stresses. A maximum static load of 13.7 KN has been applied, when it has been applied, to the Single-Stringer construction. This load has been applied continuously all the way through the duration of the construction. In the current investigation, the necessary steps have been made to explore the shear stresses that were discovered to be the result of the load in three separate planes. This was done so that conclusions can be drawn on the shear stresses. To this point, there have been a total of three distinct stages of performance that have been looked into (*XY*, *XZ*, and *ZY*). According to the conclusions of the numerical analysis, the shear stress that was applied to the *XY* plane reached a maximum of 15 MPa, whilst the shear stress that was applied to the *XZ* plane reached a maximum of 9.8 MPa. Both planes were subjected to the same amount of stress. It has reached 1.5 MPa for the plane *YZ*, despite the fact that the load that is being applied has not changed.

Fig. 13 provides a graphical illustration of the impact that shear stress has on the Single-Stringer structure. This information may be found in the above-mentioned document. The findings of the simulation indicated that the edge of the structure's core portion is the location within the structure where the shear stress is significantly higher than in any other part of the structure. The current position of view with respect to the *XZ* plane in connection with the global coordinate system. Because of the load of 13.7 kN that was placed on the specimen, the maximum value of stress, which was 9.7 MPa, was finally accomplished.

In Fig. 14, it is possible to see a visual representation of the effect that shear stress has on the Single-Stringer model. Read the aforementioned report for further details. According to the results of the simulation, shear stress is greatest at the structure's core's outside edge. Where it is looking now in relation to the *YZ* plane of the world's coordinate system. The portion of the structure that is closest to the shear plane is experiencing the greatest amount of stress. The greatest value of stress, 9.7 MPa, was reached after the specimen was subjected to a load of 13.7 kN.

The influence of shear stress on the Single-Stringer model is depicted graphically in Fig. 15. For additional information, please refer to the previously linked report. The simulation concluded that the outer edge of the core structure experienced the most shear stress. Position in the *YX* plane of the world's coordinate system at the present moment. The stress is highest in the region of the structure that is nearest the shear plane. After the specimen was loaded with 13.7 kN, the maximum stress reached 15.7 MPa.

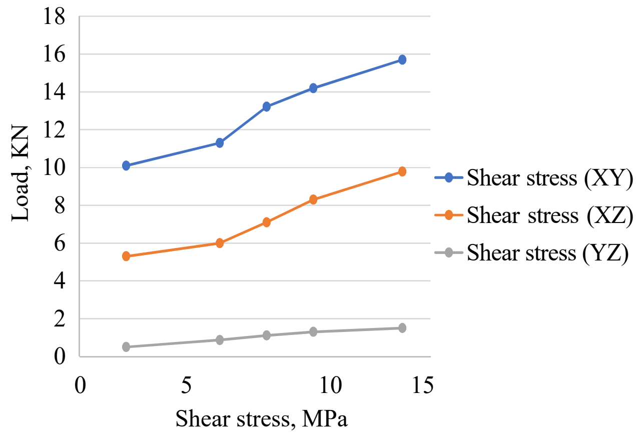

Fig. 12. Shear stress value in all planes

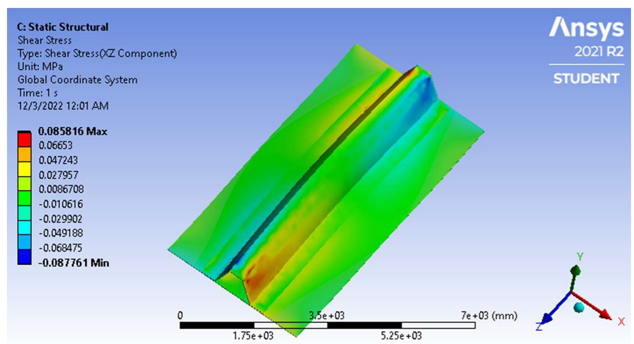

Fig. 13. shear stresses in the *XZ* plane

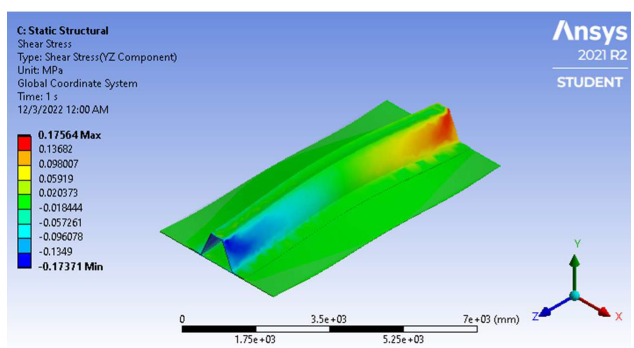

Fig. 14. shear stresses in the YZ plane

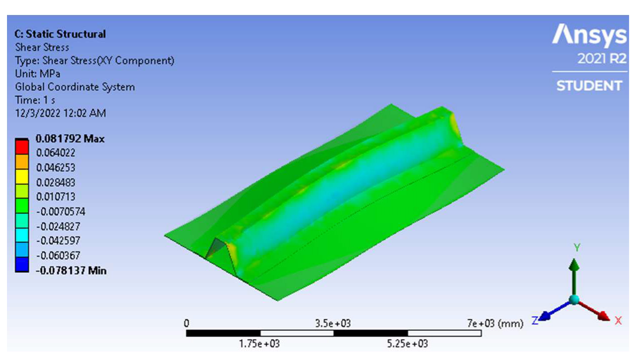

Fig. 15. shear stresses in the *XY* plane

Findings the simulation procedure has been carried out to illustrate the shear stress in three planes, and it has shown where the maximum stress is present and in which plane it is located.

6. Discussion of the investigation of the mechanical behavior of the composite single-stringer structure based on the quasi-static method

The current findings provided an explanation for the mechanical performance of the composite single-stringer construction using the quasi-static approach and the finite element method to model the static load. In order to evaluate the mechanical performance of the construction, finite element methods have been created, and the Ansys software will be used to complete the investigations.

The present numerical study of the mechanical behaviour of the composite single-stringer structure based on the quasi-static method has been validated using an experimental analysis that was carried out utilizing the apparatus that is typically used in laboratories [1].

The numerical findings of this study have been validated by examining how they stack up against the results of an earlier investigation. The corresponding elastic stress was determined by using a technique that involved a static load that remained constant. When calculating directed deformation along the X, Y, and Z axes, the findings show that the equivalent elastic stress can reach a maximum of 51.9 MPa, which is deemed to be fairly high (Fig. 10, 11). calculated along X, Y, and Z dimensions simultaneously. The calculations show that the Z-axis was subjected to the greatest amount of strain, with a value of 0.001985 mm. The total deformations along the Y-axis are 0.0143 mm, and along the X-axis, they are 0.00197 mm. The findings are presented in Fig. 6.

According to the findings of this investigation, the composite prosthetic keel experienced a total deformation when subjected to a static load. The findings of the simulation show that the maximum amount of overall deformation that can occur is 0.00058 mm, which is the minimum value that can be achieved. Calculations are made to determine the equivalent stress, or von Mises, that the static load places on the composite prosthetic keel. The findings of the inquiry into comparable elastic strain are presented graphically in Fig. 11. The results of the simulation are depicted in Fig. 12, and they indicate that the highest possible value of equivalent stress is 0.045 MPa.

As was said before, the key issue is that the numerical research of the mechanical performance of the composite prosthetic keel based on the static load has not been finished. This is the root of the majority of the problems. The modelling of this system, which helps to solve a real problem in the mechanical performance of a composite single-stringer structure, makes use of the boundary conditions that have been stated as their basis. The scope of this study is limited to a static load range of 13.7 kN and a certain kind of mesh configuration. The results of the numerical analysis that were taken into consideration are presented in excruciatingly minute detail.

There are a great number of drawbacks to consider, the most notable of which are as follows: The engineering model's mesh has room for improvement, as is currently the case.

In addition to that, an error percentage has been calculated as a result of contrasting the findings of this study with the data from the experiments. During the course of this study, a mechanism for a composite prosthetic knee was created and then subjected to numerical testing. The most challenging issue has been overcoming the challenges presented by configuring the software to accept realistic boundary limitations. There are additional restrictions, such as the manner in which new things should be defined for the program's database.

7. Conclusions

1. Total deformation of the composite single-stringer structure due to static load has been calculated. The simulation results show that the maximum value of overall deformation is 0.0147 mm.

2. Directional deformation has been calculated in three axes (X, Y and Z). The numerical results revealed that the greatest value of deformation occurred along the Z-axis, with a value of 0.001985 mm. The total deformation in the Y-axis is 0.0143 mm, as well as 0.00197 mm in the X-axis.

3. Equivalent stresses (von Mises stress) has been investigated using the approach with a static load. The maximum value of the equivalent elastic stress of 51.9 MPa has been obtained, which is considered quite high.

4. Shear stresses in three planes have been calculated, and the numerical results have showed that the XY plane has the highest value of shear stress, which is 15 MPa. This plane also has the most shear stress.

Conflict of interest

The authors declare that they have no conflict of interest in relation to this research, whether financial, personal, authorship or otherwise, that could affect the research and its results presented in this paper.

Financing

The study was performed without financial support.

Data availability

Data will be made available on reasonable request.

References

1. Raimondo, A., Doesburg, S. A., Bisagni, C. (2020). Numerical study of quasi-static and fatigue delamination growth in a post-buckled composite stiffened panel. Composites Part B: Engineering, 182, 107589. doi: https://doi.org/10.1016/j.compositesb.2019.107589
2. Zalameda, J., Winfree, W. (2018). Detection and Characterization of Damage in Quasi-Static Loaded Composite Structures using Passive Thermography. Sensors, 18 (10), 3562. doi: https://doi.org/10.3390/s18103562
3. Zalameda, J. N., Winfree, W. P., Horne, M. R. (2018). Detection of Damage During Quasi-Static Loading of a Single Stringer Panel Using Passive Thermography and Acoustic Emission. Conference Proceedings of the Society for Experimental Mechanics Series, 77–86. doi: https://doi.org/10.1007/978-3-319-95074-7_15

4. Raimondo, A., Mendez, J. P., Bisagni, C. (2021). Experimental study on post-buckled composite single-stringer specimens with initial delamination under fatigue loads. American Society for Composites 2021. doi: https://doi.org/10.12783/asc36/35772
5. Winfree, W. P., Zalameda, J. N., Horne, M. R. (2019). Simulations of thermal signatures of damage measured during quasi-static loading of a single stringer panel. AIP Conference Proceedings. doi: https://doi.org/10.1063/1.5099849
6. Milanoski, D., Galanopoulos, G., Broer, A., Zarouchas, D., Loutas, T. (2021). A Strain-Based Health Indicator for the SHM of Skin-to-Stringer Disbond Growth of Composite Stiffened Panels in Fatigue. European Workshop on Structural Health Monitoring, 626–635. doi: https://doi.org/10.1007/978-3-030-64594-6_61
7. Horne, M. R., Zalameda, J. N. (2018). Real time detection of damage during quasi-static loading of a single stringer panel using passive thermography. Thermosense: Thermal Infrared Applications XL. doi: https://doi.org/10.1117/12.2305613
8. Zalameda, J. N., Winfree, W. P., Horne, M. R. (2019). Characterization of damage formation in a composite single stringer hat stiffened panel using passive thermography. AIP Conference Proceedings. doi: https://doi.org/10.1063/1.5099753
9. Seneviratne, W., Saseendran, V., Shafie, M., Tomblin, J. (2021). Skin/stringer interface damage characterization of stiffened composite structures. American Society for Composites 2021. doi: https://doi.org/10.12783/asc36/35929
10. Milanoski, D., Galanopoulos, G., Zarouchas, D., Loutas, T. (2022). Damage Diagnostics on Post-buckled Stiffened Panels Utilizing the Digital-Twin Concept. European Workshop on Structural Health Monitoring, 213–222. doi: https://doi.org/10.1007/978-3-031-07254-3_21
11. van Dooren, K. S., Tijs, B. H. A. H., Waleson, J. E. A., Bisagni, C. (2023). Skin-stringer separation in post-buckling of butt-joint stiffened thermoplastic composite panels. Composite Structures, 304, 116294. doi: https://doi.org/10.1016/j.compstruct.2022.116294
12. Xiong, J., Zhu, Y., Luo, C., Li, Y. (2021). Fatigue-driven failure criterion for progressive damage modelling and fatigue life prediction of composite structures. International Journal of Fatigue, 145, 106110. doi: https://doi.org/10.1016/j.ijfatigue.2020.106110
13. Dogan, A. (2022). Quasi-static and dynamic response of functionally graded viscoelastic plates. Composite Structures, 280, 114883. doi: https://doi.org/10.1016/j.compstruct.2021.114883
14. Chen, J., Fang, H., Liu, W., Zhu, L., Zhuang, Y., Wang, J., Han, J. (2018). Energy absorption of foam-filled multi-cell composite panels under quasi-static compression. Composites Part B: Engineering, 153, 295–305. doi: https://doi.org/10.1016/j.compositesb.2018.08.122
15. Zha, Y., Ma, Q., Gan, X., Cai, M., Zhou, T. (2020). Deformation and energy absorption characters of Al-CFRP hybrid tubes under quasi-static radial compression. Polymer Composites, 41 (11), 4602–4618. doi: https://doi.org/10.1002/pc.25737
16. Shruti, M., Sri Hemanth, N., Badgayan, N. D., Sahu, S. K. (2021). Compressive behavior of auxetic structural metamaterial for lightweight construction using ANSYS static structural analysis. Materials Today: Proceedings, 38, 12–17. doi: https://doi.org/10.1016/j.matpr.2020.05.410
17. Mirrudula, P., Priya, P. K., Malavika, M., Kumar, G. R., Vijayanandh, R., Kumar, M. S. (2020). Comparative structural analysis of the sandwich composite using advanced numerical simulation. AIP Conference Proceedings. doi: https://doi.org/10.1063/5.0019370
18. Saravanakumar, S., Kumar Chandramohan, N., Tamil Prabakaran, S., Muniyappan, M., Shanmugam, M., Shaisundaram, V. S. (2021). The static structural analysis of torque converter material for better performance by changing the stator angle. Materials Today: Proceedings, 37, 1963–1972. doi: https://doi.org/10.1016/j.matpr.2020.07.487
19. Vijayanandh, R., Venkatesan, K., Ramesh, M., Raj Kumar, G., Senthil Kumar, M. (2019). Optimization of orientation of carbon fiber reinforced polymer based on structural analysis. International Journal of Scientific & Technology Research, 8 (11), 3020–3029. Available at: http://www.ijstr.org/final-print/nov2019/Optimization-Of-Orientation-Of-Carbon-Fiber-Reinforced-Polymer-Based-On-Structural-Analysis-.pdf
20. Htet, T. L. (2020). Structural analysis and topology design optimization of load bearing elements of aircraft fuselage structure. IOP Conference Series: Materials Science and Engineering, 709 (4), 044113. doi: https://doi.org/10.1088/1757-899x/709/4/044113
21. Carneiro, P. M. C., Gamboa, P. (2019). Structural analysis of wing ribs obtained by additive manufacturing. Rapid Prototyping Journal, 25 (4), 708–720. doi: https://doi.org/10.1108/rpj-02-2018-0044
22. Pennington, A., Goyal, V. (2023). Integration of Fatigue R-Curve Effects into VCCT for Durability Predictions, Part 1: Buckled Composite Single-Stringer Stiffened Panels. AIAA SCITECH 2023 Forum. doi: https://doi.org/10.2514/6.2023-0952
23. Martulli, L. M., Bernasconi, A. (2023). An efficient and versatile use of the VCCT for composites delamination growth under fatigue loadings in 3D numerical analysis: the Sequential Static Fatigue algorithm. International Journal of Fatigue, 170, 107493. doi: https://doi.org/10.1016/j.ijfatigue.2022.107493
24. Chiang, C.-H., Hidayat, M., Kumar, D. (2022). Simulated thermal image based on finite element models for a layered composite structures. Materials Today: Proceedings, 57, 871–877. doi: https://doi.org/10.1016/j.matpr.2022.02.539
25. Tan, R., Xu, J., Guan, Z., Sun, W., Ouyang, T., Wang, S. (2020). Experimental study on effect of impact locations on damage formation and compression behavior of stiffened composite panels with L-shaped stiffener. Thin-Walled Structures, 150, 106707. doi: https://doi.org/10.1016/j.tws.2020.106707
26. Saeedifar, M., Saleh, M. N., Nijhuis, P., de Freitas, S. T., Zarouchas, D. (2021). Damage assessment of a titanium skin adhesively bonded to carbon fiber–reinforced plastic omega stringers using acoustic emission. Structural Health Monitoring, 21 (2), 407–423. doi: https://doi.org/10.1177/14759217211001752
27. Ciminello, M., Boffa, N. D., Concilio, A., Galasso, B., Romano, F., Monaco, E. (2020). Damage Detection of CFRP Stiffened Panels by Using Cross-Correlated Spatially Shifted Distributed Strain Sensors. Applied Sciences, 10 (8), 2662. doi: https://doi.org/10.3390/app10082662